Omnidirectional Printing of 3D Microvascular Networks

*Willie Wu, Adam DeConinck, and Jennifer A. Lewis**

Nature is replete with examples of microvascular systems that enable efficient fluid flow and distribution for autonomic healing, cooling, and energy harvesting. Emulating these systems in functional materials is of considerable interest for emerging applications in self-healing,[1–3] tissue engineering,[4–7] organ printing,[8,9] microfluidics,[10,11] and biomedical devices.[12] In one example, skin-like mimics containing synthetic microvascular networks filled with healing agents demonstrated repeated repair of damage in a single location.[2,3,13] In another example, tissue engineering constructs containing both embedded cells and a planar array of microchannels were developed to facilitate the delivery of nutrient-laden fluids that promote cell viability.[14–17] Despite these recent examples, the fabrication of synthetic microvascular networks composed of complex, hierarchical 3D architectures remains an elusive goal. Although several techniques, including soft lithography,[14,18] stereolithography,[19] direct laser ablation,[20] bioprinting,[9,21] and electrostatic discharge[22] have been developed, none combine the scalability, resolution, and repeatability required to synthetically replicate 3D biomimetic microvascular constructs incorporating hierarchical, bifurcating features.

Direct ink writing (DIW) provides an attractive method for creating 3D microvascular structures due to its benign processing conditions and ease of fabrication.[3,10,13,23] In this method, a fugitive organic ink is patterned into the desired motif, encapsulated in a thermally or photocurable resin, and subsequently removed by liquefication to yield a microvascular network consisting of uniform microchannels interconnected in three dimensions. As originally implemented, its layer-by-layer build sequence limits network designs to simple architectures, such as those based on 3D periodic lattices. Recently, Hansen et al.[24] used dual fugitive inks in combination with vertical printing to create 3D interpenetrating microvascular networks. While these advances permit increased pattern complexity, even this modified approach is unable to create true 3D biomimetic microvascular networks.

Here, we demonstrate the omnidirectional printing (ODP) of 3D biomimetic microvascular networks (**Figure 1**); a new variant of direct-write assembly that vastly broadens the network design space by obviating the need for layerwise patterning. In this approach, fugitive ink filaments are printed within a photocurable gel reservoir, which physically supports the patterned features thereby allowing truly omnidirectional freeform fabrication (Figure 1a). As the deposition nozzle translates through the reservoir, void space is generated locally and filled by the migration of liquid from the fluid capping layer (Figure 1b). The liquid filler is designed to have identical chemical functionality, yet a significantly lower viscosity than the photopolymerizable reservoir. Thus, any voids produced during printing are immediately filled. After printing is completed, the gel reservoir and fluid filler are solidified via photo-polymerization to form a mechanically robust, chemically crosslinked matrix (Figure 1c). Because the fugitive ink has not been chemically modified, it can be subsequently removed by liquefication at 4 °C under a modest vacuum to yield the desired microchannel network within the matrix (Figure 1d,e).

To enable ODP of 3D biomimetic microvascular networks, we developed a chemically compatible fugitive ink, fluid filler, and physical gel reservoir, whose properties are tailored for printing and subsequent transformation into the desired structures. Specifically, we created a fluorescently dyed, fugitive ink composed of an aqueous solution of Pluronic F127, a triblock copolymer with a hydrophobic poly(propylene oxide) (PPO) segment and two hydrophilic poly(ethylene oxide) (PEO) segments arranged in a PEO-PPO-PEO configuration and a diacrylate-functionalized Pluronic F127 solution[25–27] of varying concentration as the fluid filler and physical gel reservoir, respectively.[28] Using this system, we constructed 3D biomimetic microvascular networks composed of a hierarchical, 3-generation branching topology with microchannel diameters ranging from 200–600 μm, in which two large parent channels are subdivided into many smaller microchannels (Figure 1f).

Aqueous Pluronic F127 triblock copolymer solutions undergo a phase transition that is both concentration and temperature dependent.[29–31] Under ambient conditions, the PEO-PPO-PEO species form micelles that consist of a PPO core surrounded by a PEO corona above a critical micelle concentration (CMC) of ~21 w/w% yielding a physical gel, as reflected by the substantial increase in shear elastic modulus, G' as the concentration exceeds the CMC (**Figure 2**a). As reported previously, these spherical micelles have an average hydrodynamic diameter ranging from 20–80 nm.[29] In addition, these Pluronic F127 solutions also possess a critical micelle temperature (CMT) of ~10 °C (Figure 2b). Above the CMT, the PPO block dehydrates leading to pronounced hydrophobic interactions that drive micelle formation. However, below the CMT, the hydrophobic PPO units are hydrated, allowing individual PEO-PPO-PEO species to become soluble in water thereby inducing a gel-to-fluid transition for systems, whose concentration resides above the CMC. Concomittantly, there is an abrupt decrease in G' at temperatures below ~10 °C.

We exploit the known phase behavior of aqueous Pluronic F127 solutions in the design of our ink, matrix, and fluid filler. Our fugitive ink consists of an aqueous solution of Pluronic F127 that resides slightly above the CMC. This ink exhibits pronounced shear thinning behavior (Figure S1, Supporting Information) and shear elastic plateau modulus G' that exceeds

W. Wu, A. DeConinck, Prof. J. A. Lewis
Department of Materials Science and Engineering
University of Illinois at Urbana-Champaign
Urbana, IL 61801, USA
E-mail: jalewis@illinois.edu

DOI: 10.1002/adma.201004625

© 2011 WILEY-VCH Verlag GmbH & Co. KGaA, Weinheim

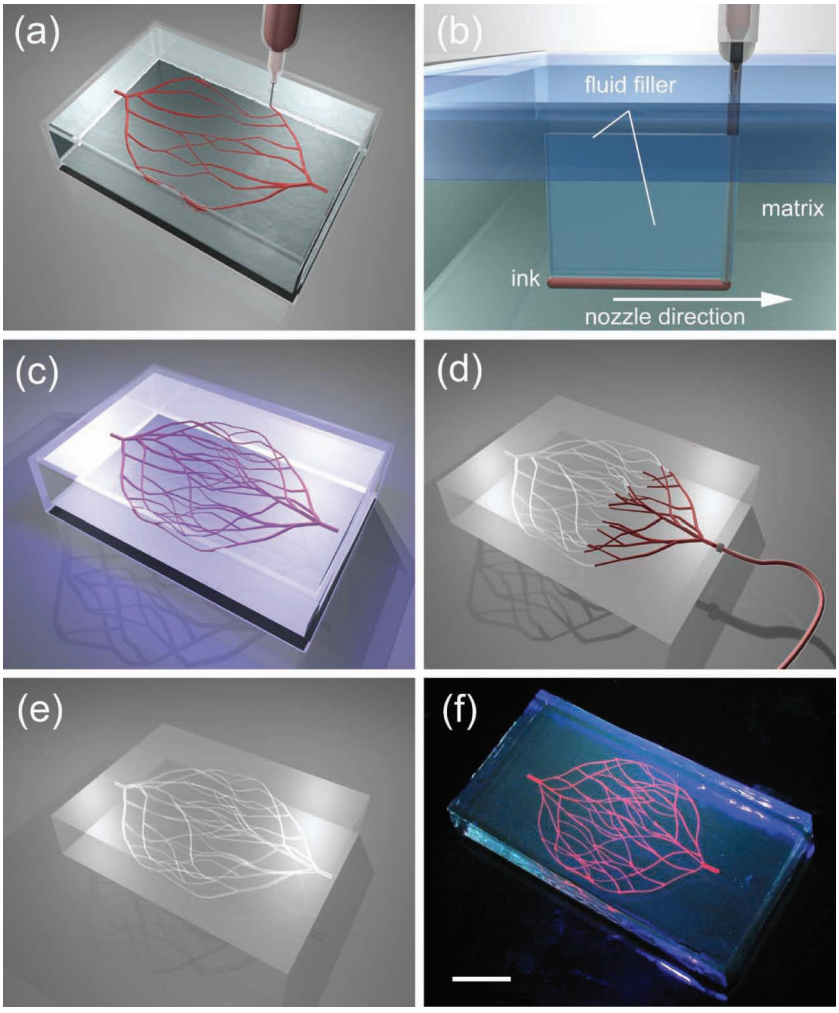

Figure 1. a–e) Schematics of omnidirectional printing of 3D microvascular networks within a hydrogel reservoir. a) Deposition of a fugitive ink into a physical gel reservoir allows hierarchical, branching networks to be patterned. b) Voids induced by nozzle translation are filled with liquid that migrates from the fluid capping layer. c) Subsequent photopolymerization of the reservoir yields a chemically cross-linked, hydrogel matrix. d,e) The ink is liquified and removed under a modest vacuum to expose the microvascular channels. f) Fluorescent image of a 3D microvascular network fabricated via omnidirectional printing of a fugitive ink (dyed red) within a photopolymerized Pluronic F127-diacrylate matrix. (scale bar = 10 mm)

10^4 Pa (Figure 2a). This rheological response allows the ink to be extruded through a fine nozzle, while maintaining its filamentary form after patterning is completed. However, when the temperature is reduced below the critical micelle temperature (<10 °C), the ink liquefies and G' decreases by several orders of magnitude (Figure 2b). We rely on this phase change to remove the patterned ink features from the three-dimensional matrix in which they are embedded.

The design of an appropriate supporting hydrogel reservoir and filler fluid poses several challenges. To enable ODP, the reservoir must exhibit a high plateau shear elastic modulus, G', to support the patterned ink filaments, a low yield stress, τ_y, to accommodate nozzle translation, and the ability to be chemically cross-linked after printing. While pure Pluronic F127 solutions can be tailored to satisfy the first two criteria, they are not robust enough to allow ink removal. To meet this latter criteria, we chemically modified the terminal hydroxyl groups of the PEO segments with diacrylate groups.[29–31] In its chemically modified, uncured state, Pluronic F127 diacrylate (F127-DA) solutions exhibit a CMC of 23 w/w% (Figure 2c), which is slightly higher than their non-functionalized counterpart. We used a F127-DA gel that possesses a viscosity and G' similar to that of the pure fugitive ink (Figure S1, Supporting Information). Importantly, this reservoir can be photopolymerized to produce a chemically cross-linked matrix by incorporating a photoinitiator followed by irradiation of 365 nm UV light for 5 min.

During ODP, the nozzle translates through the uncured Pluronic F127-DA gel to deposit fugitive ink in the desired 3D microvascular network pattern. As this process occurs, void spaces are introduced into the matrix. To fill these crevasses, we used a fluid filler composed of a liquid solution of the acrylate-modified Pluronic F127, which is placed on top of the matrix as a capping layer (1 mm thick). Because its concentration lies below the CMC, the fluid filler exhibits Newtownian behavior under ambient conditions with a viscosity of 6.6×10^{-1} Pa s^{-1} and a negligible shear elastic modulus (Figure 2c). However, since the filler fluid is chemically identical to the supporting reservoir, it can be photocured after patterning of the 3D microvascular network is complete.

Next, we investigated the printing behavior of the fugitive ink, hydrogel reservoir, and fluid filler over a range of compositions to determine their respective optimal formulations for ODP. Our assessment of ink performance included the ability to cleanly start and stop ink flow, to control the microchannel diameter by dynamic pressure variation, and to retain its filamentary shape during and after deposition. We also assessed the reservoir and fluid filler performance; the reservoir must support the deposited ink filaments without disuption due to viscous drag as the nozzle translates through nearby regions, while the fluid must rapidly fill gaps formed within the reservoir during the patterning process. Optimal concentrations of ~23 w/w% for the ink and 25 w/w% reservoir were determined for ODP (Figure 2d), both of which reside above their respective critical micelle concentrations of 21 w/w% and 23 w/w% (Figure 2a,b). Fluid inks exhibited drop-breakup leading to the formation of discontinuous filaments. For this ink/reservoir combination, a minimum ink elastic modulus of $>10^4$ Pa is required for filamentary printing. The maximum concentration of Pluronic F127 that can be dissolved in water is 30 w/w%, which represents an upper bound.

To control the microchannel diameter, we employed a dynamic pressure variation approach in which a single nozzle

© 2011 WILEY-VCH Verlag GmbH & Co. KGaA, Weinheim

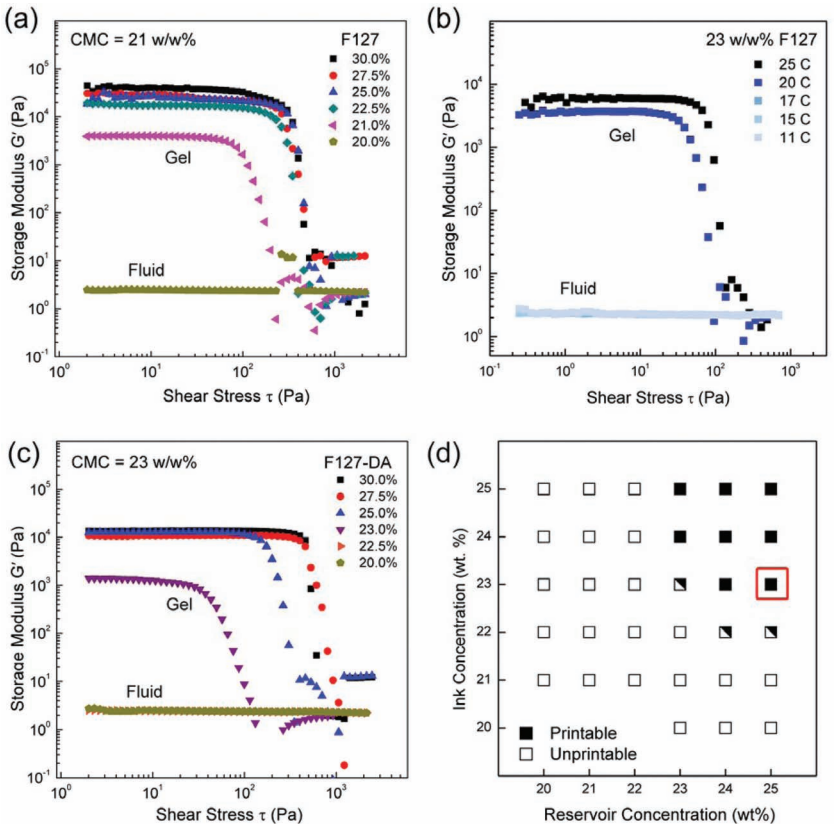

Figure 2. a) Log-log plot of the shear elastic modulus, G' as a function of shear stress τ for Pluronic F127 at 25 °C. b) Log-log plot of the ink elasticity as a function of shear stress for Pluronic F127 at varying temperatures. (c) Log-log plot of the shear elastic modulus, G' as a function of shear stress τ for Pluronic F127-diacrylate at 25 °C. d) Printing performance as a function of varying ink and reservoir concentrations, which denotes printable (solid squares), borderline (half-squares), and unprintable (open squares) compositions. The red box denotes optimal formulations for omnidirectional printing.

is used to pattern microchannels of varying size. When the applied pressure (P) and writing speed (v) are controlled such that the volumetric flow rate (Q) equals $0.25\pi D_{nozzle}^2 v$, the microchannel diameter ($D_{channel}$) is nearly equal to the nozzle diameter (D_{nozzle}). However, this approach would require the use of multiple nozzles to pattern hierarchical, bifurcating microchannels.[23] To overcome this limitation, we varied the applied pressure at a constant writing speed. We observed a linear increase in the microchannel diameter with applied pressure for fugitive ink deposition into the hydrogel reservoir (**Figure 3**a). While this trend is consistent, we found that the slope varied with nozzle diameter. For example, microchannels with diameters ranging from 18 μm to 170 μm ($D_{channel}$ ~0.5 to 5.5D_{nozzle}, respectively) could be achieved using a 30 μm tapered glass capillary (Figure 3b,c), which is the smallest nozzle through which this ink readily flows. Although features slightly smaller than the nozzle diameter were obtained, further reductions in the applied pressure led to filament breakup. Microchannels of up to 600 μm ($D_{channel} = 3D_{nozzle}$) could be formed using a 200 μm cylindrical stainless steel nozzle. However, this does not constitute an upper bound, since larger microchannels (>1 mm) can be produced simply by using a large nozzle size (see Supplementary Movie 1, Supporting Information).

To examine effect of initial reservoir and filler fluid composition on the final mechanical properties of the cured Pluronic F127-DA matrix, we performed dynamical mechanical analysis of 1″ circular specimens to obtain their elastic modulus E' as a function of concentration. Unlike the strong concentration dependence observed for G', the mechanical properties (E') of the cured system depends only modestly on concentration (Figure 3d). This finding indicates that E' is influenced primarily by the formation of a chemically crosslinked matrix rather than its initial physical gel or fluid state. Hence, the incorporation of fluid filler within the reservoir during omnidirectional printing does not adversely affect the final mechanical properties of the bulk matrix.

Hydrogel matrices with embedded 3D biomimetic microvascular networks may find potential application in tissue engineering[32] and drug delivery.[33] In these applications, the diffusion rate of solutes from fluid-filled microchannels into the surrounding matrix imposes additional design constraints on the microvascular network. For example, in cell-seeding applications,[14–17] nutrient diffusion is limited to several hundred microns,[34] which dictates in part the maximum allowable microchannel spacing. To characterize the diffusivity (D) of a low molecular weight solute within the cross-linked Pluronic F127-DA matrix, we injected a rhodamine-based fluorescent dye into a 125 μm microchannel and allowed it to diffuse into the matrix under quiescent conditions (**Figure 4**a). The diffusion profile acquired by fluorescent imaging consists of averaged intensities normalized to $t* = 0$ (Figure 4b) and shows the progression of the dye through the matrix. For the image analysis, the intensity is assumed to be proportional to the concentration. The spatial peak variance, σ^2, is extracted from 1D Gaussian fits from each profile with $R^2 > 0.98$, excluding the channel region. Using the Einstein-Smoluchowski relation, the diffusion constant is determined from the plot of σ^2 as a function of time (Figure 4c). Specifically, we found a diffusion constant $D = 2.15 \times 10^{-7}$ cm^2 s^{-1} for a 0.1 w/w% dye in a 25 w/w% Pluronic F127-DA matrix. As a control, we verified the validity of this approach using an agar system, where the measured diffusivity was consistent with reported values (see Supporting Information).

In summary, we have fabricated 3D biomimetic microvascular networks embedded within a hydrogel matrix via omnidirectional printing. This novel approach hinges critically on tailoring the chemical and rheological properties of the fugitive ink as well as the photopolymerizable hydrogel reservoir and fluid filler. These hydrogel-based, microvascular constructs may find potential application in 3D cell culture, tissue

© 2011 WILEY-VCH Verlag GmbH & Co. KGaA, Weinheim

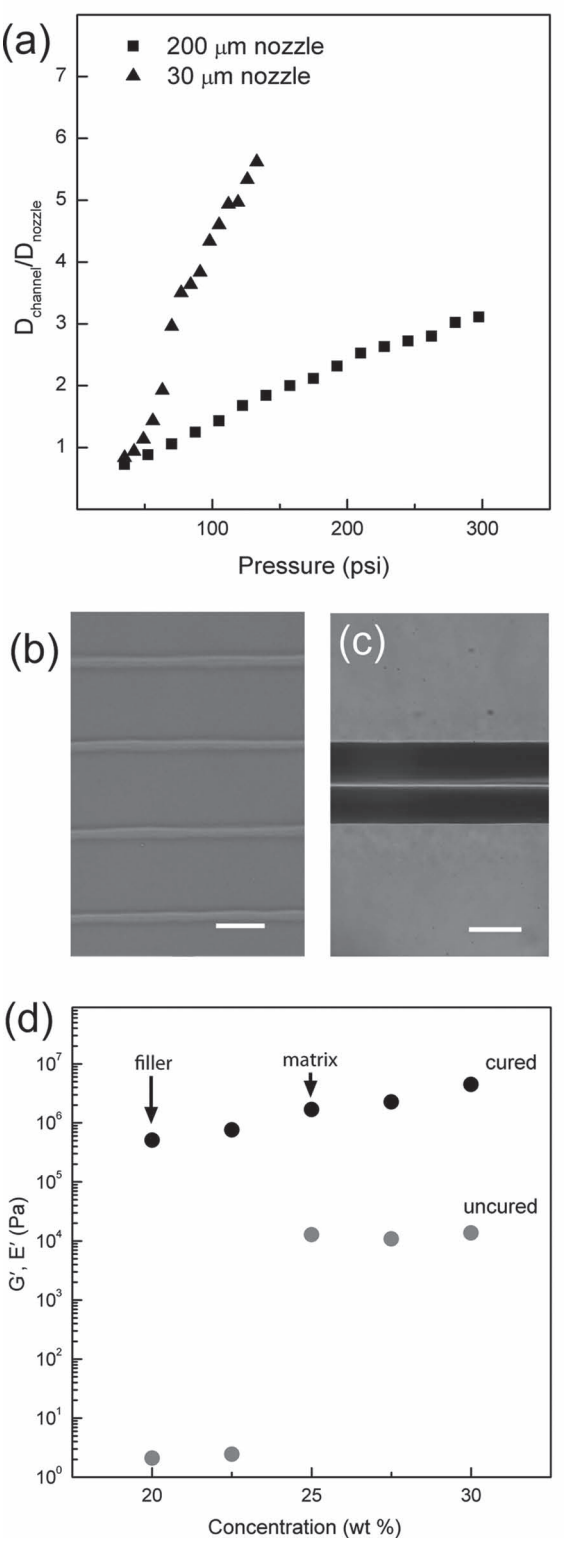

Figure 3. a) Normalized microchannel diameter as a function of applied pressure at a printing speed of 6 mm s^{-1} using a (■) 200 μm cylindrical stainless steel nozzle and a (▲) 30 μm tapered glass capillary. Optical images of printed b) 18 μm and c) 175 μm microchannels (scale bars = 100 μm). d) Shear elastic modulus G' of uncured Pluronic F127-DA (●, gray symbols) and compressive modulus E' of the cured (●, black symbols) Pluronic F127-DA as a function of concentration.

engineering, organ modeling, or autonomic healing. Looking ahead, this approach may be readily extended to create complex 3D composites by incorporating nanoparticles or other functional building blocks within the ink, reservoir, or both components of the system.

Experimental Section

Preparation of the Pluronic F127 Fugitive Ink: The fugitive ink is produced by dissolving Pluronic F127 (Sigma-Aldrich) into 4 °C deionized water at 23 w/w% and stirring vigorously for 3 h. Several drops of a water-soluble fluorescent dye are added to the ink to aid in visualization during omnidirectional printing. The solution is stored overnight in a refrigerator to allow air bubbles to dissipate. The cooled ink is poured into 5 mL syringes (EFD-Inc) and warmed to room temperature prior to printing.

Synthesis of Pluronic F127-DA: 100 g of Pluronic F127 (Sigma-Aldrich) is dissolved into 400 ml of dry toluene at 60 °C in a oven-dried three-neck round-bottom flask fitted with a condenser with circulating cold (20 °C) water to minimize solvent evaporation. The solution is allowed to cool to room temperature using an ice bath under a dry nitrogen flow. Triethylamine (Sigma-Aldrich) is added to the solution at a molar ratio of 10:1 Pluronic F127-DA while stirring. Acryloyl chloride (Sigma-Aldrich) at a molar ratio of 10:1 Pluronic F127-DA is added to the flask drop-wise, and the reaction is allowed to proceed while stirring overnight at 25 °C under nitrogen. The yellow triethylammonium hydrochloride is filtered and the remaining Pluronic F127-DA solution is precipitated in a 1:1 ratio of hexane. The final product is filtered and dried at room temperature for 24 h.

Preparation of Pluronic F127-DA Fluid Filler and Matrix: The Pluronic F127-DA fluid filler and matrix is prepared at 20 and 25 w/w% respectively by mixing in cold water and stirring vigorously for 3 hrs. 1 w/w% of a photoinitiator (Dargocure 1173, Ciba) is added, and the solution is then allowed to defoam in a refrigerator overnight.

Omnidirectional Printing: 3D microvascular branched networks are fabricated using a three-axis robotic deposition stage (ABL9000, Aerotech Inc.) by printing a 3D pattern into a physical gel reservoir. The 3D patterns are designed using commercially available CAD software (AutoCAD 2010, Autodesk) and translated into G-code instructions for the deposition stage using a custom Visual Basic program. The 23 w/w% Pluronic F127 ink is housed in a 5 mL syringe fitted with nozzles ranging in size from 10 μm to 200 μm (World Precision Instruments and Nordson EFD). Prior to deposition, a reservoir of 25 w/w% Pluronic F127-DA is poured into a silicone mold at 4 °C and slowly solidified by warming to room temperature, inducing the formation of micelles. The nozzle tip is inserted into the bottom of the gel reservoir and a 1 mm thick layer of a 20 w/w% Pluronic F127-DA filler fluid is poured on top of the gel reservoir prior to printing. Air pressure (Ultimus V, Nordson EFD) is applied to initiate extrusion. The ink filament size is varied dynamically, by first printing calibration standards that consist of arrays of parallel channels at various pressures and measuring their printed dimensions by optical microscopy. From these data, the linear relationship between applied pressure and filament size was determined. After deposition, the Pluronic F127-DA is chemically cross-linked under 365 nm UV light for 5 minutes. The ink is subsequently removed by exposing the largest (parent) channels with a razor blade, cooling the structure under ice water, and applying a light vacuum.

Characterization of Rheology and Mechanical Properties: The rheological properties of aqueous Pluronic F127 and F127-DA solutions of varying concentration are measured using a controlled-stress rheometer (Bohlin CVOR-200, Malvern Instruments) fitted with a C14 cup and bob geometry. 2.5 mL of the solutions are poured into the geometry at 4 °C and allowed to equilibrate to room temperature. Oscillatory-shear measurements are carried out at 1 Hz with a stress amplitude range of 0.1 to 2000 Pa. Viscometry measurements are performed at a shear rate of 0.01 to 100 s^{-1}. Dynamic mechanical

© 2011 WILEY-VCH Verlag GmbH & Co. KGaA, Weinheim

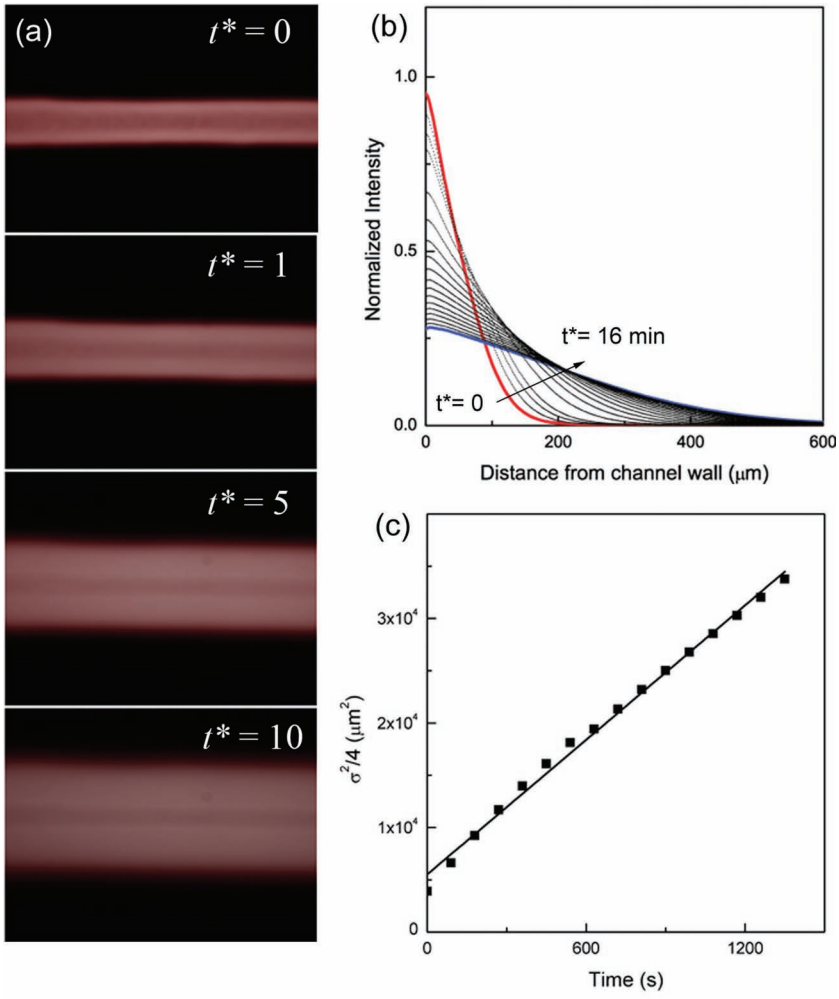

Figure 4. Diffusion of a rhodamine-based dye through photocured Pluronic F127-DA. a) Fluorescent images of microchannels (120 μm in diameter) at $t* = 0$, 1, 5, and 10 min, where $t* = 0$ designates the time that the first image is taken after dye injection. b) Diffusion profiles of the fluorescent intensity normalized to the maximum at $t* = 0$. c) The spatial peak variance σ^2 obtained from Gaussian fits of the intensity profiles plotted as a function of time, from which the slope yields a dye diffusivity of 2.15×10^{-7} cm^2 s^{-1}.

analysis is performed on cured Pluronic F127-DA gels at 20, 22.5, 25, 27.5, and 30 w/w%. Circular discs with a diameter of 1″ and thickness of 2 mm are cured for 5 min before mounting onto a dynamic mechanical analyzer (RSA3, TA Instruments) fitted with parallel plates. The elastic compressive modulus E' is measured at a frequency of 1 Hz and a strain of 0.5%.

Determination of ODP Deposition Parameters: Several screening tests are used to establish optimal rheological parameters of the ink, fluid filler, and matrix over the concentration range from 20–25 w/w% Pluronic F127 and F127-DA, respectively. All specimens are cured under 365 nm UV light and qualitatively examined by optical microscopy. A printable ink possessed clean breaks in filaments without tailing during stops/starts, channel size scalability with applied pressure, and shape retention throughout the entire process. An acceptable matrix supported the filaments without introducing filament breakup due to viscous drag induced by nozzle translation during the printing process.

Transport Properties of F127-DA: A static imaging technique is used to characterize the diffusion constants of small molecular weight species through the cross-linked Pluronic F127-DA matrix. Microchannels (125 μm diameter and length of 20 mm) are printed in a 25 w/w% F127-DA matrix. A 0.1 w/w% water soluble rhodamine-based dye (FWT Red, Bright Dyes. MW~500) is injected into the microchannel and allowed to diffuse into the surrounding matrix. Fluorescent images are acquired using an inverted fluorescence microscope (Leica DMI 6000B) at specific time intervals and analyzed in MATLAB. Diffusion profiles are obtained by averaging the fluorescent intensities and normalizing to the maximum intensity at time $t* = 0$, the time at which the first image is acquired after dye injection. We assume that the fluorescence intensity is directly proportional to the concentration, and that the dye exhibits 1D Fickian diffusion:[35]

$$C(x,t) = \frac{N/A}{\sqrt{4\pi Dt}} \exp\left(\frac{-(x - x_0)^2}{4Dt}\right) \quad (1)$$

where C is the dye concentration, N is the number of dye molecules, A is the cross-sectional area through which they diffuse, x_0 is the position of the line source along the x axis, perpendicular to the channel length, D is the diffusion constant, and t is the time. Using the Einstein-Smoluchowski relation

$$\sigma^2 = 2Dt \quad (2)$$

where σ^2 is the spatial peak variance, the equation can be rewritten as a standard Gaussian function:

$$C(x,t) = \frac{N/A}{\sqrt{2\pi\sigma^2}} \exp\left(\frac{-(x - x_0)^2}{2\sigma^2}\right) \quad (3)$$

At each time step, the fluorescent intensity profile is fitted to a Gaussian function in MATLAB to obtain the fitting parameter σ^2, the spatial peak variance. Shadow regions caused by a mismatch in the index of refraction were omitted from the fit. The diffusion constant is determined from slope of σ^2 plotted as a function of diffusion time, t.

Supporting Information

Supporting Information is available from the Wiley Online Library or from the author.

Acknowledgements

The authors gratefully acknowledge funding for this project provided by AFOSR Multidisciplinary University Research Initiative (Grant # FA9550–05-1–0346) led by S. R. White.

Received: December 16, 2010
Revised: February 15, 2011
Published online: March 23, 2011

[1] S. R. White, N. R. Sottos, P. H. Geubelle, J. S. Moore, M. R. Kessler, S. R. Sriram, E. N. Brown, S. Viswanathan, *Nature* **2001**, *409*, 794.
[2] K. S. Toohey, N. R. Sottos, J. A. Lewis, J. S. Moore, S. R. White, *Nat. Mater.* **2007**, *6*, 581.

© 2011 WILEY-VCH Verlag GmbH & Co. KGaA, Weinheim

[3] C. J. Hansen, W. Wu, K. S. Toohey, N. R. Sottos, S. R. White, J. A. Lewis, *Adv. Mater.* **2009**, *21*, 4143.
[4] R. Langer, J. Vacanti, *Science* **1993**, *260*, 920.
[5] J. Borenstein, E. Weinberg, B. Orrick, C. Sundback, M. Kaazempur-Mofrad, J. Vacanti, *Tissue Eng.* **2007**, *13*, 1837.
[6] J. T. Borenstein, H. Terai, K. R. King, E. J. Weinberg, M. R. Kaazempur-Mofrad, J. P. Vacanti, *Biomed. Microdev.* **2002**, *4*, 167.
[7] A. P. Golden, J. Tien, *Lab Chip* **2007**, *7*, 720.
[8] N. E. Fedorovich, J. Alblas, J. R. de Wijn, W. E. Hennink, A. J. Verbout, W. J. A. Dhert, *Tissue Eng.* **2007**, *13*, 1905.
[9] C. Norotte, F. S. Marga, L. E. Niklason, G. Forgacs, *Biomaterials* **2009**, *30*, 5910.
[10] D. Therriault, S. R. White, J. A. Lewis, *Nat. Mater.* **2003**, *2*, 265.
[11] T. D. Wheeler, A. D. Stroock, *Nature* **2008**, *455*, 208.
[12] T. Fujii, *Microelectron. Eng.* **2002**, *61–62*, 907.
[13] K. S. Toohey, C. J. Hansen, J. A. Lewis, S. R. White, N. R. Sottos, *Adv. Funct. Mater.* **2009**, *19*, 1399.
[14] N. W. Choi, M. Cabodi, B. Held, J. P. Gleghorn, L. J. Bonassar, A. D. Stroock, *Nat. Mater.* **2007**, *6*, 908.
[15] Y. Ling, J. Rubin, Y. Deng, C. Huang, U. Demirci, J. M. Karp, A. Khademhosseini, *Lab Chip* **2007**, *7*, 756.
[16] M. Cabodi, N. W. Choi, J. P. Gleghorn, C. S. D. Lee, L. J. Bonassar, A. D. Stroock, *J. Am. Chem.Soc.* **2005**, *127*, 13788.
[17] J. H. Park, B. G. Chung, W. G. Lee, J. Kim, M. D. Brigham, J. Shim, S. Lee, C. M. Hwang, N. G. Durmus, U. Demirci, A. Khademhosseini, *Biotechnol. Bioeng.* **2010**, *106*, 138.
[18] A. Khademhosseini, R. Langer, J. Borenstein, J. P. Vacanti, *Proc. Nat. Acad.Sci. USA* **2006**, *103*, 2480.
[19] C. Xia, N. Fang, *Biomed. Microdev.* **2009**, *11*, 1309.
[20] D. Lim, Y. Kamotani, B. Cho, J. Mazumder, S. Takayama, *Lab on a Chip* **2003**, *3*, 318.
[21] C. Gentile, P. Fleming, J. Zhang, R. P. Visconti, C. J. Visconti, V. Mironovi, *Int. J. Artif. Organs* **2008**, *31*, 583.
[22] J. H. Huang, *Adv. Mater.* **2009**, *21*, 3567.
[23] W. Wu, C. J. Hansen, A. M. Aragon, P. H. Geubelle, S. R. White, J. A. Lewis, *Soft Matter* **2010**, *6*, 739.
[24] C. J. Hansen, W. Wu, K. S. Toohey, N. R. Sottos, S. R. White, J. A. Lewis, *Adv. Mater.* **2009**, *21*, 4143.
[25] A. Sosnik, D. Cohn, Rom, J. S. n, G. A. Abraham, *J. Biomater. Sci., Polym. Ed.* **2003**, *14*, 227.
[26] N. Sanabria-DeLong, A. J. Crosby, G. N. Tew, *Biomacromolecules* **2008**, *9*, 2784.
[27] K. T. Nguyen, J. L. West, *Biomaterials* **2002**, *23*, 4307.
[28] E. Hecht, H. Hoffmann, *Langmuir* **1994**, *10*, 86.
[29] M. Bohorquez, C. Koch, T. Trygstad, N. Pandit, *J. Colloid Interface Sci.* **1999**, *216*, 34.
[30] P. Linse, M. Malmsten, *Macromolecules* **1992**, *25*, 5434.
[31] G. E. Yu, Y. L. Deng, S. Dalton, Q. G. Wang, D. Attwood, C. Price, C. Booth, *J. Chem. Soc. Faraday Trans.* **1992**, *88*, 2537.
[32] D. M. Hoganson, H. I. Pryor, 2nd, I. D. Spool, O. H. Burns, J. R. Gilmore, J. P. Vacanti, *Tissue Eng. Part A* **2010**, *16*, 1469.
[33] T. R. Hoare, D. S. Kohane, *Polymer* **2008**, *49*, 1993.
[34] Y. Martin, P. Vermette, *Biomaterials* **2005**, *26*, 7481.
[35] C. T. Culbertson, S. C. Jacobson, J. Michael Ramsey, *Talanta* **2002**, *56*, 365.

© 2011 WILEY-VCH Verlag GmbH & Co. KGaA, Weinheim